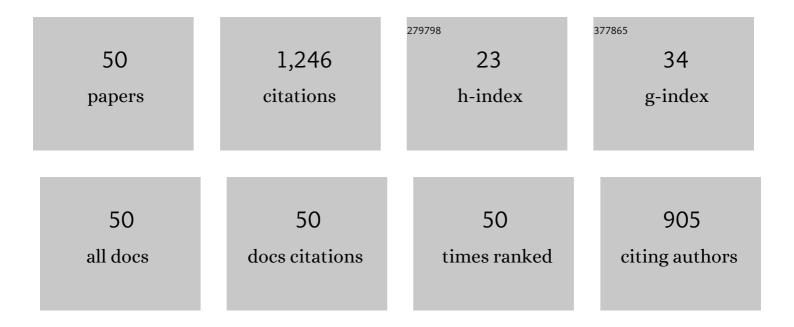
## Firman M Simanjuntak

List of Publications by Year in descending order

Source: https://exaly.com/author-pdf/6945162/publications.pdf Version: 2024-02-01



#	Article	IF	CITATIONS
1	Flexible Ta <sub>2</sub> O <sub>5</sub> /WO <sub>3</sub> -Based Memristor Synapse for Wearable and Neuromorphic Applications. IEEE Electron Device Letters, 2022, 43, 9-12.	3.9	14
2	Negative Effects of Annealed Seed Layer on the Performance of ZnO-Nanorods Based Nitric Oxide Gas Sensor. Sensors, 2022, 22, 390.	3.8	5
3	Formation of a ternary oxide barrier layer and its role in switching characteristic of ZnO-based conductive bridge random access memory devices. APL Materials, 2022, 10, 031103.	5.1	2
4	Effects of Surface Polarity on the Structure and Magnetic Properties of Epitaxial <i>h</i> -YMnO <sub>3</sub> Thin Films Grown on MgO Substrates. ACS Applied Electronic Materials, 2022, 4, 1603-1610.	4.3	3
5	ZrOX insertion layer enhanced switching and synaptic performances of TiOX-based memristive devices. IOP Conference Series: Materials Science and Engineering, 2021, 1034, 012142.	0.6	0
6	Evaluating gallium-doped ZnO top electrode thickness for achieving a good switch-ability in ZnO2/ZnO bilayer transparent valence change memory. Journal of Electroceramics, 2021, 46, 14-19.	2.0	2
7	Band tailoring by annealing and current conduction of Co-doped ZnO transparent resistive switching memory. IOP Conference Series: Materials Science and Engineering, 2021, 1034, 012140.	0.6	0
8	Conduction mechanism of Co-doped ZnO transparent memristive devices. IOP Conference Series: Materials Science and Engineering, 2021, 1034, 012139.	0.6	0
9	Transformation of digital to analog switching in TaOx-based memristor device for neuromorphic applications. Applied Physics Letters, 2021, 118, .	3.3	37
10	Negative effect of cations out-diffusion and auto-doping on switching mechanisms of transparent memristor devices employing ZnO/ITO heterostructure. Applied Physics Letters, 2021, 118, .	3.3	7
11	Low-power electronic technologies for harsh radiation environments. Nature Electronics, 2021, 4, 243-253.	26.0	39
12	Crafting the multiferroic BiFeO <sub>3</sub> -CoFe <sub>2</sub> O <sub>4</sub> nanocomposite for next-generation devices: A review. Materials and Manufacturing Processes, 2021, 36, 1579-1596.	4.7	19
13	Conduction channel configuration controlled digital and analogÂresponse in TiO <sub>2</sub> -based inorganic memristive artificial synapses. APL Materials, 2021, 9, 121103.	5.1	5
14	Effects of pillar size modulation on the magneto-structural coupling in self-assembled BiFeO <sub>3</sub> –CoFe <sub>2</sub> O <sub>4</sub> heteroepitaxy. CrystEngComm, 2020, 22, 435-440.	2.6	12
15	Barrier Layer Induced Switching Stability in Ga:ZnO Nanorods Based Electrochemical Metallization Memory. IEEE Nanotechnology Magazine, 2020, 19, 764-768.	2.0	15
16	Fast, Highly Flexible, and Transparent TaO <sub><i>x</i></sub> -Based Environmentally Robust Memristors for Wearable and Aerospace Applications. ACS Applied Electronic Materials, 2020, 2, 3131-3140.	4.3	30
17	Suboxide interface induced digital-to-analog switching transformation in all Ti-based memristor devices. Applied Physics Letters, 2020, 117, .	3.3	18
18	Neutral oxygen irradiation enhanced forming-less ZnO-based transparent analog memristor devices for neuromorphic computing applications. Nanotechnology, 2020, 31, 26LT01.	2.6	36

Firman M Simanjuntak

#	Article	IF	CITATIONS
19	Stress Corrosion Cracking Threshold for Dissimilar Capacitive Discharge Welding Joint with Varied Surface Geometry. Applied Sciences (Switzerland), 2020, 10, 2180.	2.5	3
20	Sensing performance of gas sensors fabricated from controllably grown ZnO-based nanorods on seed layers. Journal of Materials Science, 2020, 55, 8850-8860.	3.7	19
21	Synthesis of Fe3O4/Ag nanohybrid ferrofluids and their applications as antimicrobial and antifibrotic agents. Heliyon, 2020, 6, e05813.	3.2	30
22	Improving linearity by introducing Al in HfO <sub>2</sub> as a memristor synapse device. Nanotechnology, 2019, 30, 445205.	2.6	86
23	Corrosion Inhibition of Honeycomb Waste Extracts for 304 Stainless Steel in Sulfuric Acid Solution. Materials, 2019, 12, 2120.	2.9	16
24	Influence of rf sputter power on ZnO film characteristics for transparent memristor devices. AIP Advances, 2019, 9, .	1.3	25
25	Film-Nanostructure-Controlled Inerasable-to-Erasable Switching Transition in ZnO-Based Transparent Memristor Devices: Sputtering-Pressure Dependency. ACS Applied Electronic Materials, 2019, 1, 2184-2189.	4.3	32
26	Enhanced Synaptic Linearity in ZnO-Based Invisible Memristive Synapse by Introducing Double Pulsing Scheme. IEEE Transactions on Electron Devices, 2019, 66, 4722-4726.	3.0	49
27	ZnO2/ZnO bilayer switching film for making fully transparent analog memristor devices. APL Materials, 2019, 7, .	5.1	44
28	Switching and synaptic characteristics of AZO/ZnO/ITO valence change memory device. IOP Conference Series: Materials Science and Engineering, 2019, 494, 012027.	0.6	4
29	Synthesis and Electrochemical Performance of α-Fe2O3 Nano Ellipse as Anode for Lithium-Ion Batteries. Asian Journal of Chemistry, 2019, 31, 487-492.	0.3	1
30	Role of precursors mixing sequence on the properties of CoMn2O4 cathode materials and their application in pseudocapacitor. Scientific Reports, 2019, 9, 16852.	3.3	20
31	Neutral Oxygen Beam Treated ZnO-Based Resistive Switching Memory Device. ACS Applied Electronic Materials, 2019, 1, 18-24.	4.3	31
32	The impact of TiW barrier layer thickness dependent transition from electro-chemical metallization memory to valence change memory in ZrO2-based resistive switching random access memory devices. Thin Solid Films, 2018, 660, 777-781.	1.8	25
33	Controlled resistive switching characteristics of ZrO <sub>2</sub> -based electrochemical metallization memory devices by modifying the thickness of the metal barrier layer. Japanese Journal of Applied Physics, 2018, 57, 04FE10.	1.5	23
34	Resistive switching behavior of Ga doped ZnO-nanorods film conductive bridge random access memory. Thin Solid Films, 2018, 660, 828-833.	1.8	31
35	Switching Failure Mechanism in Zinc Peroxide-Based Programmable Metallization Cell. Nanoscale Research Letters, 2018, 13, 327.	5.7	26
36	Structural and electrical properties analysis of InAlGaN/GaN heterostructures grown at elevated temperatures by MOCVD. Journal of Crystal Growth, 2018, 501, 7-12.	1.5	8

#	Article	IF	CITATIONS
37	Resistive Switching Characteristics of Hydrogen Peroxide Surface Oxidized ZnO-Based Transparent Resistive Memory Devices. ECS Transactions, 2017, 77, 155-160.	0.5	18
38	Role of nanorods insertion layer in ZnO-based electrochemical metallization memory cell. Semiconductor Science and Technology, 2017, 32, 124003.	2.0	30
39	One bipolar transistor selector - One resistive random access memory device for cross bar memory array. AIP Advances, 2017, 7, .	1.3	29
40	Peroxide induced volatile and non-volatile switching behavior in ZnO-based electrochemical metallization memory cell. Nanotechnology, 2017, 28, 38LT02.	2.6	28
41	Effect of barrier layer on switching polarity of ZrO2-based conducting-bridge random access memory. Applied Physics Letters, 2017, 111, .	3.3	25
42	Resistive Switching Characteristics of Hydrogen Peroxide Surface Oxidized ZnO-Based Transparent Resistive Memory Devices. ECS Meeting Abstracts, 2017, , .	0.0	0
43	Impacts of Co doping on ZnO transparent switching memory device characteristics. Applied Physics Letters, 2016, 108, .	3.3	70
44	Temperature induced complementary switching in titanium oxide resistive random access memory. AIP Advances, 2016, 6, 075314.	1.3	31
45	Status and Prospects of ZnO-Based Resistive Switching Memory Devices. Nanoscale Research Letters, 2016, 11, 368.	5.7	188
46	Enhanced switching uniformity in AZO/ZnO1â^²x/ITO transparent resistive memory devices by bipolar double forming. Applied Physics Letters, 2015, 107, .	3.3	52
47	Enhancing the memory window of AZO/ZnO/ITO transparent resistive switching devices by modulating the oxygen vacancy concentration of the top electrode. Journal of Materials Science, 2015, 50, 6961-6969.	3.7	55
48	Electrospinning Processing and Microstructural Characterization of Ce <sub>0.78</sub> Gd <sub>0.2</sub> Sr <sub>0.02</sub> O <sub>2-Î</sub> Fiber for a Composite Anode. Advanced Materials Research, 2011, 287-290, 2489-2493.	0.3	0
49	Practical Approach to Induce Analog Switching Behavior in Memristive Devices: Digital-to-Analog Transformation. , 0, , .		1
50	Transparent ZnO resistive switching memory fabricated by neutral oxygen beam treatment. Japanese Journal of Applied Physics, 0, , .	1.5	2